PHYSICAL REVIEW A VOLUME 28, NUMBER 3 SEPTEMBER 1983

Theory of light scattering in cholesteric blue phases

R. M. Hornreich and S. Shtrikman
Department of Electronics, Weizmann Institute of Science, Rehovot 76100, Israel
(Received 29 November 1982)

A comprehensive analysis of elastic light scattering in cholesteric liquid-crystal systems, based upon the Mueller matrix approach, is given. Emphasis is placed upon analyzing the polarization state of the scattered light for arbitrarily polarized incident radiation. The theory is applied to the ordered cholesteric blue phases BPI and BPII, which exhibit long-range orientational ordering. Both the polycrystalline and single-crystal cases are considered and the role played by optical activity is studied. It is shown how light-scattering studies yield information on the structural properties of the ordered phases. The quasielastic light scattering due to excitations in the disordered phase is also analyzed in the harmonic approximation. It is shown that this scattering cannot explain the strong anomolous scattering observed in the amorphous BPIII phase.

I. INTRODUCTION

The blue phases (BP) which appear in a narrow temperature range in many cholesteric liquid crystals just below their clearing point are currently being intensively investigated experimentally[1–12] and theoretically.[13–19] Two of these phases, which have been named BPI and BPII, exhibit sharp Bragg peaks in the optical region of the spectrum.[1–3(b),5(b),10] These peaks can be indexed on cubic unit cells and this, together with other evidence,[1,4,7(b),11(a)] has resulted in general acceptance of cubic structures for BPI and BPII. However, since the limited number of Bragg peaks observed to date can be indexed on either body-centered (bcc) or simple cubic (sc) unit cells, definite space group assignments have not as yet been possible. (Morphological studies[7(b),11(a)] indicate that BPI and BPII are most probably bcc and sc, respectively.) Moreover, after this basic point is resolved one would like to go further and assign these cubic phases to specific space groups.

In an earlier paper,[13(d)] we pointed out that the fact that BP Bragg scattering occurs in the optical rather than the x-ray regime provides additional means for resolving the above questions. The reason for this is the following: at x-ray wavelengths, the high energy of the incident radiation results in pure scalar scattering, i.e., the interaction is essentially one in which the incident beam is scattered by free electrons. At optical wavelengths, however, the much lower energy of the incident radiation results in scattering, in addition, by all components of the tensor order parameter. In other words, the BP structure factor, which determines the selection rules for the Bragg scattering or arbitrarily polarized light, now has a tensor rather than scalar character.

Recently, a detailed presentation of the Landau theory of cholesteric systems and the blue phases was given.[13(h)] Using this theoretical framework, we here present a comprehensive analysis of elastic light scattering in cholesterics. We consider the general case in which the incident beam has arbitrary polarization properties and show how a study of the scattered light can yield information on the structural properties of the liquid crystal. Both the ordered BP and the disordered (isotropic) phases are discussed. Our analysis utilizes the Mueller matrix formalism,[20] which is particularly suitable in the present case from both the theoretical and experimental points of view.

In Sec. II, we first present those aspects of the Landau theory directly relevant to the study of light scattering in cholesterics. We then introduce the Mueller matrix formalism and calculate the matrix characterizing Bragg scattering by an ordered polycrystalline specimen. The resulting expression is compared with experimental results.[2(b),3(d)] Next, we discuss the role of optical activity and calculate the Mueller matrix appropriate to this case. Again, comparison with reported experimental data[3(d)] is made. We conclude this section by analyzing the case of Bragg scattering by a single-crystal specimen. This approach could be useful for detecting relatively weak components of the BP order parameter. The reason for this is that such components enter into the Mueller matrix linearly in the single-crystal case, but only quadratically in the polycrystalline case.

In Sec. III, we analyze quasielastic scattering in the isotropic phase, again using the Mueller matrix formalism. We restrict ourselves to the harmonic approximation, in which only fluctuations quadratic in the order parameter and its spatial derivatives are considered. The results are compared with those found experimentally in amorphous BPIII, the "gray" or "fog" phase observed in some liquid crystals in a very narrow temperature interval (~ 0.1 K) between the isotropic and cubic phases. Finally, in Sec. IV, we summarize our results and indicate some promising lines for further study.

II. THE MUELLER MATRIX FORMALISM: SCATTERING IN THE ORDERED PHASE

A. General considerations

In cholesteric liquid crystals, typical molecular dimensions are of the order of 10 Å while optical wavelengths are of the order of 10^3 Å. Thus, at optical wavelengths, continuum models of elastic scattering are excellent approximations and this framework will be used by us here. In a continuum theory, the elastic scattering of light is, in general, a consequence of spatial variations in the dielectric tensor, $\epsilon_{ij}^d(\vec{r};\omega)$. Assuming that we are interested in frequencies ω which are far away from any absorption bands, only the real part of the dielectric tensor is of interest and we henceforth regard ϵ_{ij}^d as real. In this case, ϵ_{ij}^d is symmetric and can, in principle, be regarded as a linear combination of six basis tensors. Since we are interested in structural periodic ordered phases, it will be convenient to expand $\epsilon_{ij}^d(\vec{r};\omega)$ in Fourier components. We first separate the isotropic and anisotropic parts of ϵ_{ij}^d by writing

$$\epsilon_{ij}^d(\vec{r}) \equiv \epsilon_{ij} + \tfrac{1}{3}\,\mathrm{Tr}(\epsilon^d)\delta_{ij} = \epsilon_{ij} + \bar{\epsilon}\delta_{ij} \ . \tag{1}$$

The anisotropic part ϵ_{ij} is generally taken as the order parameter.[21] In Fourier components

$$\epsilon_{ij}^d(\vec{r}) = \sum_{h,k,l} N^{-1/2}\epsilon_{ij}(\sigma)\exp[iq(hx+ky+lz)] + \sum_{h,k,l} N^{-1/2}\bar{\epsilon}(\sigma)\delta_{ij}\exp[iq(hx+ky+lz)] \ , \tag{2}$$

where $\sigma = h^2+k^2+l^2$ and N is the multiplicity of $\langle hkl \rangle$. In general $N = 3!2^{3-n_0}/n_1!$, where n_0 (n_1) is the number of vanishing (equal) $|h|, |k|, |l|$. The wave vector q, which is related to the unit cell size, is determined by minimizing the system's free energy.[13(a)–13(c),13(e),13(h)] For each (hkl) [including (000)], we have

$$\begin{aligned}\underline{\epsilon}(\sigma) &= \sum_{m=-2}^{2} \epsilon_m(\sigma)e^{i\psi_m(hkl)}\underline{M}_m(hkl) \\ &= \frac{1}{2}\left[\epsilon_2 e^{i\psi_2}\begin{bmatrix}1 & i & 0\\ i & -1 & 0\\ 0 & 0 & 0\end{bmatrix} + \epsilon_1 e^{i\psi_1}\begin{bmatrix}0 & 0 & 1\\ 0 & 0 & i\\ 1 & i & 0\end{bmatrix} + \sqrt{2/3}\epsilon_0 e^{i\psi_0}\begin{bmatrix}-1 & 0 & 0\\ 0 & -1 & 0\\ 0 & 0 & 2\end{bmatrix}\right. \\ &\quad \left. + \epsilon_{-1}e^{i\psi_{-1}}\begin{bmatrix}0 & 0 & -1\\ 0 & 0 & i\\ -1 & i & 0\end{bmatrix} + \epsilon_{-2}e^{i\psi_{-2}}\begin{bmatrix}1 & -i & 0\\ -i & -1 & 0\\ 0 & 0 & 0\end{bmatrix}\right] ,\end{aligned} \tag{3}$$

with $\epsilon_m(\sigma) \geq 0$ and $\psi_m(hkl) = -\psi_m(\bar{h}\bar{k}\bar{l})$. The basis matrices $\underline{M}_m$ are defined such that (hkl) is along the polar axis of a local coordinate system, which is defined uniquely for each (hkl). Note that certain of the $\epsilon_m(\sigma)$ will necessarily vanish for specific space groups[13(d),13(h)] and that the phases $\psi_m(hkl)$ are determined uniquely (modulo π) by the space-group symmetry.[13(h)] The nonvanishing amplitudes $\epsilon_m(\sigma)$ can all be determined, in principle, from a minimization of the Landau free-energy functional.[21] This has been done, however, only in a limited number of cases.[13(a)–13(c),13(e),13(h),14,17(b)]

B. Bragg scattering in polycrystals

A systemic description of the scattering of arbitrarily polarized radiation by a linear medium is provided by the Mueller matrix formalism.[20] In this approach, we describe the properties of the input and output beams in terms of 4×1 column matrices known as Stokes vectors or parameters. The connection between these vectors can then be expressed as a linear transformation whose 16 coefficients[22] form the 4×4 Mueller matrix. The usefulness of this particular approach follows from the principle of optical equivalence, which states that it is impossible to distinguish between incoherent sums of simple waves which form beams having identical Stokes vectors by the use of optical instrumentation. Thus, in practice, the Stokes vector, which characterizes the intensity and state of polarization of a beam of light, contains all quantities of physical interest. The effect of a linearly scattering medium is to

change the Stokes vector and this change is described by the appropriate Mueller matrix. Note that since the scattering process in liquid crystals can result in partial depolarization of the incident beam, the Jones or coherency matrix approach is not adequate.

We are here primarily interested in calculating the Mueller matrix describing the Bragg scattering of light at a wave vector $Q=q\sqrt{\sigma}$ for the case of a liquid crystal composed of randomly orientated ordered crystallities. Our notation is summarized schematically in Fig. 1. Here k_α and k_β are the wave vectors of the incoming and outgoing light beams, respectively, and $\vec{Q}=\vec{k}_\beta-\vec{k}_\alpha$ is the scattering wave vector. For elastic scattering $|\vec{k}_\alpha|=|\vec{k}_\beta|=k_0$ and the scattering half-angle θ is given by

$$\sin\theta=Q/2k_0 \ . \tag{4}$$

With each of the wave vectors in Fig. 1(a) we associate a local right-handed coordinate system, having its z axis along the wave vector and its x axis in the scattering plane as shown in Fig. 1(b). The incoming beam can be regarded as a linear combination of plane waves, each having a transverse electric field vector of the form

$$\vec{\mathscr{E}}_\alpha=\vec{E}_\alpha\exp[i(k_0z_\alpha-\omega t+\delta_\alpha)]+\text{c.c.} \ , \tag{5a}$$

with

$$\vec{E}_\alpha=E_{\alpha1}\hat{1}_\alpha+E_{\alpha2}\hat{2}_\alpha \ . \tag{5b}$$

Here c.c. denotes the associated complex conjugate and the $\hat{n}_\alpha$ are unit vectors defining the incoming-beam local coordinate system. The phases δ_α are, in general, independent and uncorrelated. Transforming to the frame of the scattering wave vector, (5b) becomes

$$\vec{E}_\alpha=-E_{\alpha1}\sin\theta\,\hat{1}_Q+E_{\alpha2}\hat{2}_Q+E_{\alpha1}\cos\theta\,\hat{3}_Q \ , \tag{6}$$

with $\hat{n}_Q$ the relevant unit vectors.

For *each* incoming plane wave, there will be a Bragg-scattered wave whose electric field will be proportional, in first-order Born approximation (i.e., neglecting multiple scattering contributions) to the product of the $\pm Q$ Fourier components of $\epsilon^d_{ij}(\vec{r})$ and the incoming electric field. Each scattered wave thus has the form

$$\vec{\mathscr{E}}_\beta=\vec{E}_\beta\exp[i(k_0z_\beta-\omega t+\delta_\alpha)] \ . \tag{7}$$

Using (2), (3), and (6), the electric-field-vector amplitude $\vec{E}_\beta$ scattered from a single incoming plane wave in a particular crystallite whose local x axis is at an angle ϕ_Q to $\hat{1}_Q$ (by construction, the z axes coincide) becomes in the $\hat{n}_Q$ coordinate frame

$$\begin{bmatrix}E_{\beta1}\\E_{\beta2}\\E_{\beta3}\end{bmatrix}=\tfrac{1}{2}g\begin{bmatrix}2\tilde{\epsilon}+\epsilon_2\alpha_2-\epsilon_0\alpha_0+\epsilon_{-2}\alpha_{-2} & i(\epsilon_2\alpha_2-\epsilon_{-2}\alpha_{-2}) & \epsilon_1\alpha_1-\epsilon_{-1}\alpha_{-1}\\ i(\epsilon_2\alpha_2-\epsilon_{-2}\alpha_{-2}) & 2\tilde{\epsilon}-\epsilon_2\alpha_2-\epsilon_0\alpha_0-\epsilon_{-2}\alpha_{-2} & i(\epsilon_1\alpha_1+\epsilon_{-1}\alpha_{-1})\\ \epsilon_1\alpha_1-\epsilon_{-1}\alpha_{-1} & i(\epsilon_1\alpha_1+\epsilon_{-1}\alpha_{-1}) & 2(\tilde{\epsilon}+\epsilon_0\alpha_0)\end{bmatrix}\begin{bmatrix}-E_{\alpha1}\sin\theta\\E_{\alpha2}\\E_{\alpha1}\cos\theta\end{bmatrix} \ , \tag{8a}$$

with

$$\alpha_{\pm m}=e^{i(\psi_{\pm m}\pm m\phi_\alpha)}, \quad m=1,2$$
$$\alpha_0=\sqrt{2/3}e^{i\psi_0} \ . \tag{8b}$$

The proportionality factor g in 8(a) will be discussed later in this section.

We now express $\vec{E}_\beta$ in the outgoing coordinate frame, defined by the unit vectors $\hat{n}_\beta$. We have

$$\vec{E}_\beta=E_{\beta1}\hat{1}_\beta+E_{\beta2}\hat{2}_\beta+E_{\beta3}\hat{3}_\beta \ , \tag{9a}$$

and the transverse (to $\vec{k}_\beta$) amplitudes are given by

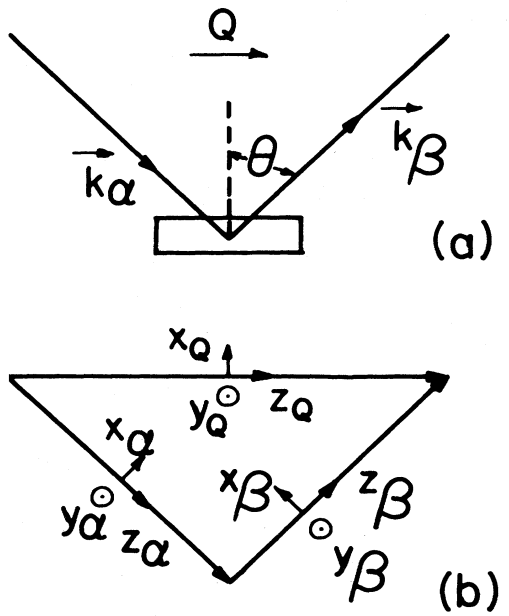

FIG. 1. (a) Schematic view of the scattering plane, showing the wave vectors characterizing the incident ($\vec{k}_\alpha$) and scattered ($\vec{k}_\beta$) light beams and the scattering wave vector $\vec{Q}$. (b) The local coordinate systems associated, respectively, with each of the three wave vectors.

$$E_{\beta 1}=\tfrac{1}{2}g\{[2\tilde{\epsilon}c_2-(\epsilon_2\alpha_2+\epsilon_{-2}\alpha_{-2})s^2+\epsilon_0\alpha_0(c^2+1)]E_{\alpha 1}+i[(\epsilon_2\alpha_2-\epsilon_{-2}\alpha_{-2})s+(\epsilon_1\alpha_1+\epsilon_{-1}\alpha_{-1})c]E_{\alpha 2}\}\ ,$$
$$E_{\beta 2}=\tfrac{1}{2}g\{-i[(\epsilon_2\alpha_2-\epsilon_{-2}\alpha_{-2})s-(\epsilon_1\alpha_1+\epsilon_{-1}\alpha_{-1})c]E_{\alpha 1}+(2\tilde{\epsilon}-\epsilon_2\alpha_2-\epsilon_0\alpha_0-\epsilon_{-2}\epsilon_{-2})E_{\alpha 2}\}\ . \tag{9b}$$

We have simplified our notation by setting $c=\cos\theta$, $s=\sin\theta$, $c_2=\cos(2\theta)$, and $s_2=\sin(2\theta)$.

Rather than calculating the Stokes vectors directly, it is convenient to first consider the corresponding Jones or coherency matrices. For the outgoing beam, we also sum over all the randomly oriented crystallites, obtaining the polycrystalline Jones matrix

$$\langle \underline{J}\rangle_\phi \equiv \begin{bmatrix} \sum\langle E_{\beta 1}E^*_{\beta 1}\rangle_\phi \\ \sum\langle E_{\beta 1}E^*_{\beta 2}\rangle_\phi \\ \sum\langle E^*_{\beta 1}E_{\beta 2}\rangle_\phi \\ \sum\langle E_{\beta 2}E^*_{\beta 2}\rangle_\phi \end{bmatrix}\ , \tag{10a}$$

where by $\sum$ we understand a sum over all the plane waves composing the output beam and the angular brackets with subscript ϕ denote an integral over all azimuthal orientations ϕ. $\langle \underline{J}_\beta\rangle_\phi$ is linearly related to the Jones matrix $\underline{J}_\alpha$ of the incoming beam, which is, of course, given by

$$\underline{J}_\alpha \equiv \begin{bmatrix} \sum E_{\alpha 1}E^*_{\alpha 1} \\ \sum E_{\alpha 1}E^*_{\alpha 2} \\ \sum E^*_{\alpha 1}E_{\alpha 2} \\ \sum E_{\alpha 2}E^*_{\alpha 2} \end{bmatrix}\ . \tag{10b}$$

We write the linear relationship between $\langle \underline{J}_\beta\rangle_\phi$ and $\underline{J}_\alpha$ in the form

$$\langle \underline{J}_\beta\rangle_\phi=\tfrac{1}{4}g^2\underline{T}\underline{J}_\alpha\ , \tag{11a}$$

where the elements of the 4×4 Hermitian matrix $\underline{T}$ are, from (9b) and (10),

$$\begin{aligned}
T_{11}&=|2\tilde{\epsilon}c_2+\epsilon_0\alpha_0(c^2+1)|^2+(\epsilon_2^2+\epsilon_{-2}^2)s^4\ ,\\
T_{12}&=-T_{21}=-T_{13}=T_{31}=i(\epsilon_2^2-\epsilon_{-2}^2)s^3\ ,\\
T_{14}&=T_{41}=(\epsilon_2^2+\epsilon_{-2}^2)s^2+(\epsilon_1^2+\epsilon_{-1}^2)c^2\ ,\\
T_{22}&=T^*_{33}=[2\tilde{\epsilon}c_2+\epsilon_0\alpha_0(c^2+1)](2\tilde{\epsilon}-\epsilon_0\alpha_0^*)\\
&\quad+(\epsilon_2^2+\epsilon_{-2}^2)s^2\ ,\\
T_{23}&=T_{32}=-(\epsilon_2^2+\epsilon_{-2}^2)s^2+(\epsilon_1^2+\epsilon_{-1}^2)c^2\ ,\\
T_{24}&=-T_{42}=-T_{34}=T_{43}=-i(\epsilon_2^2-\epsilon_{-2}^2)s\ ,\\
T_{44}&=|2\tilde{\epsilon}-\epsilon_0\alpha_0|^2+(\epsilon_2^2+\epsilon_{-2}^2)\ .
\end{aligned} \tag{11b}$$

The Stokes (column) vectors $\underline{S}_\alpha$ and $\langle \underline{S}_\beta\rangle_\phi$ for the incoming and outgoing beams, respectively, are related to the corresponding Jones matrices by the linear transformation

$$\underline{S}_\alpha=\underline{A}\underline{J}_\alpha, \langle \underline{S}_\beta\rangle_\phi=\underline{A}\langle \underline{J}_\beta\rangle_\phi\ , \tag{12a}$$

where $\underline{A}$ is a 4×4 matrix whose elments are

$$\begin{aligned}
A_{11}&=A_{14}=A_{21}=-A_{24}=A_{32}=A_{23}=iA_{42}\\
&=-iA_{43}=1\ ,\\
A_{12}&=A_{13}=A_{22}=A_{23}=A_{31}=A_{34}=A_{41}\\
&=A_{44}=0\ .
\end{aligned} \tag{12b}$$

Thus, e.g., the Stokes vector for the incoming beam is

$$\underline{S}_\alpha=\begin{bmatrix} S_{\alpha 1}\\ S_{\alpha 2}\\ S_{\alpha 3}\\ S_{\alpha 4}\end{bmatrix}=\begin{bmatrix} \sum(E_{\alpha 1}E^*_{\alpha 1}+E_{\alpha 2}E^*_{\alpha 2})\\ \sum(E_{\alpha 1}E^*_{\alpha 1}-E_{\alpha 2}E^*_{\alpha 2})\\ \sum(E_{\alpha 1}E^*_{\alpha 2}+E^*_{\alpha 1}E_{\alpha 2})\\ -i\sum(E_{\alpha 1}E^*_{\alpha 2}-E^*_{\alpha 1}E_{\alpha 2})\end{bmatrix}\ . \tag{13}$$

Before completing the derivation of the Mueller matrix for Bragg scattering, we digress to give a brief physical interpretation of the parameters S_n $(n=1,\ldots,4)$ composing the Stokes (column) vector. In all cases, S_1 is simply proportional to the total intensity of the beam. The other parameters, however, depend upon other beam properties. Consider, for example, a single monochromatic plane wave. In this case, only three of the S_n are independent, since

$$S_1^2=S_2^2+S_3^2+S_4^2\ . \tag{14a}$$

If the wave is linearly polarized, $S_4=0$ and $\arctan(S_3/S_2)$ is the angle between the wave's $\vec{E}$ field and the x axis. If the wave is right $(+)$ or left $(-)$ circularly polarized, then $S_2=S_3=0$ and $S_4=\pm S_1$.

For the case of unpolarized (e.g., natural) light, the Stokes (column) vector has the form $[S_1,0,0,0]$. More generally, when the beam is a quasimonochromatic plane wave composed of independent polarized and unpolarized portions, (14a) must be replaced by the general relation

$$S_1^2\geq S_2^2+S_3^2+S_4^2\ , \tag{14b}$$

with the equality holding only for the pure monochromatic case.

Experimentally, S_1 can be measured by taking the

sum of the intensities transmitted by two ideal linear polarizers, aligned with the x and y axes, respectively. S_2 is then simply the difference between these two quantities. If the above experiment is repeated, but with the polarizers now aligned along $\pm\pi/4$, the difference in the measured intensities will be S_3. Finally, if the linear polarizers are replaced by circular ones, S_4 will be the difference between intensities passed by the right- and left-handed polarizers.

We now return to our derivation of the Mueller matrix $\underline{\mu}_p$ for elastic Bragg scattering by a polycrystalline specimen. It is defined implicitly by the relation

$$\langle \underline{S}_\beta \rangle_\phi = \underline{\mu}_p \underline{S}_\alpha \ . \tag{15}$$

Using (11a) and (12a), we have, from (15),

$$\underline{\mu}_p = \tfrac{1}{4} g^2 \underline{A} \underline{T} \underline{A} \underline{T}^{-1} \ . \tag{16}$$

Since (16) is a unitary transformation, it follows that $\underline{\mu}_p$ is also Hermitian. Introducing the reduced matrix

$$\underline{\tilde{\mu}} = \underline{\mu}_p / \tfrac{1}{8} g^2 \ , \tag{17a}$$

we obtain, from (11b), (12b), and (16),

$$\begin{aligned}
&\tilde{\mu}_{11} = |\, 2\tilde{\epsilon} c_2 + \epsilon_0 \alpha_0 (c^2+1) \,|^2 + |\, 2\tilde{\epsilon} - \epsilon_0 \alpha_0 \,|^2 + (\epsilon_2^2 + \epsilon_{-2}^2)(s^2+1)^2 + 2(\epsilon_1^2 + \epsilon_{-1}^2) c^2 \ , \\
&\tilde{\mu}_{12} = \tilde{\mu}_{21} = |\, 2\tilde{\epsilon} c_2 + \epsilon_0 \alpha_0 (c^2+1) \,|^2 - |\, 2\tilde{\epsilon} - \epsilon_0 \alpha_0 \,|^2 - (\epsilon_2^2 + \epsilon_{-2}^2)(1 - s^4) \ , \\
&\tilde{\mu}_{13} = \tilde{\mu}_{31} = \tilde{\mu}_{23} = \tilde{\mu}_{32} = 0 \ , \\
&\tilde{\mu}_{14} = \tilde{\mu}_{41} = -2(\epsilon_2^2 - \epsilon_{-2}^2) s (s^2+1) \ , \\
&\tilde{\mu}_{22} = |\, 2\tilde{\epsilon} c_2 + \epsilon_0 \alpha (c^2+1) \,|^2 + |\, 2\tilde{\epsilon} - \epsilon_0 \alpha_0 \,|^2 + (\epsilon_2^2 + \epsilon_{-2}^2) c^4 - 2(\epsilon_1^2 + \epsilon_{-1}^2) c^2 \ , \\
&\tilde{\mu}_{24} = \tilde{\mu}_{42} = 2(\epsilon_2^2 - \epsilon_{-2}^2) s c^2 \ , \\
&\tilde{\mu}_{33} = 2\,\mathrm{Re}\{[2\tilde{\epsilon} c_2 + \epsilon_0 \alpha_0 (c^2+1)](2\tilde{\epsilon} - \epsilon_0 \alpha_0^*)\} + 2(\epsilon_1^2 + \epsilon_{-1}^2) c^2 \ , \\
&\tilde{\mu}_{34} = -\tilde{\mu}_{43} = 2i\,\mathrm{Im}\{[2\tilde{\epsilon} c_2 + \epsilon_0 \alpha_0 (c^2+1)](2\tilde{\epsilon} - \epsilon_0 \alpha_0^*)\} \ , \\
&\tilde{\mu}_{44} = 2\,\mathrm{Re}\{[2\tilde{\epsilon} c_2 + \epsilon_0 \alpha_0 (c^2+1)](2\tilde{\epsilon} - \epsilon_0 \alpha_0^*)\} + 4(\epsilon_2^2 + \epsilon_{-2}^2) s^2 - 2(\epsilon_1^2 + \epsilon_{-1}^2) c^2 \ .
\end{aligned} \tag{17b}$$

Experimentally, it is convenient to consider a modified version of (15) in which the relationship is between the differential scattered intensity matrix $\underline{\Phi}$ (in units of energy per unit time per unit halo length) and the input beam flux $\underline{I}$ (in units of energy per unit area per unit time). Since these quantities are proportional to $\langle \underline{S}_\beta \rangle_\phi$ and $\underline{S}_\alpha$, respectively, we can absorb the associated proportionality factors into g^2 and rewrite (15) as

$$\underline{\Phi} = \tfrac{1}{8} \tilde{g}^2 \underline{\tilde{\mu}} \underline{I} \ . \tag{18}$$

To determine $\tilde{g}^2$ for scattering by a polycrystalline specimen, we consider the case of pure scalar scattering by density variations. In this case, only $\tilde{\epsilon} \neq 0$ in (17b), and we have

$$\Phi_1 = \tfrac{1}{8} \tilde{g}^2 \mu_{11} I_1 = \tfrac{1}{2} \tilde{g}^2 \tilde{\epsilon}^2 I_1 (1 + c_2^2) \ . \tag{19}$$

This relation can also be derived directly from standard results for Debye-Scherrer scattering by a polycrystalline specimen and the coefficient $\tilde{g}$ determined by comparison. The relevant equations are[23]

$$\begin{aligned}
&dP/dl = \Phi_1 = I_1 \bar{N} Y V / 8\pi r s \ , \\
&Y = \tfrac{1}{2} \lambda^3 \rho^2 \,|\, F \,|^2 (e^2/mc^2)^2 (1 + c_2^2)/s_2 \ , \\
&F(hkl) = \sum_j f_j \exp[-iq(hx_j + ky_j + lz_j)] \ .
\end{aligned} \tag{20}$$

The notation in (20) is as follows: dP is the energy per unit time scattered into a halo segment of length $dl = r\,d\phi$; $\bar{N}$ is the number of diffracting planes scattering into the angle between 2θ and $2(\theta + d\theta)$. Here $\bar{N} = N$, the multiplicity factor; r is the distance from the specimen to the plane of the halo (the observation plane)—thus $l = 2\pi r s_2$ is the halo length; V is the specimen volume; ρ is the density (number per unit volume) of crystallographic unit cells; λ is the wavelength (in the material) of the incoming beam—it is related to the scattering wave vector $\vec{Q}$ and scattering half-angle θ by Bragg's law, $Q = 4\pi s/\lambda$; e, m, and c are the electronic charge and mass, and the speed of light, respectively; F the structure factor, is the Fourier sum over a unit cell of the scattering amplitudes f_j of the individual atomic scatterers located at positions (x_j, y_j, z_j) within the cell.

For scalar scattering at high frequencies, the atomic dielectric polarization

$$(\epsilon_a)_{ij}=\epsilon_a\delta_{ij}$$

is related to the scattering amplitude f by

$$\epsilon_a=(4\pi e^2/m\omega^2)f \ . \tag{21}$$

Taking a Fourier sum over a unit cell and using $\omega=2\pi c/n\lambda$, where n is the index of refraction, (21) becomes

$$VN^{-1/2}\tilde{\epsilon}(\sigma)=(n^2\lambda^2/\pi)(e^2/mc^2)(F/\rho V) \ , \tag{22}$$

where ρV is just the total number of crystallographic unit cells. The differential scattered intensity parameter Φ_1 is thus given by

$$\Phi_1=(\pi N^2\tilde{\epsilon}^2V/32rn^4\lambda s^2c)I_1(1+c_2^2) \ . \tag{23}$$

Comparing (19) and (23), we find

$$\tilde{g}^2=\pi N^2V/16rn^4\lambda s^2c \ . \tag{24}$$

Equations (17b), (18), and (24) comprise the central results of our analysis in this section.

We now consider several particular cases of the Mueller matrix for Bragg scattering by a polycrystalline specimen. In general, density variations will be negligible compared with those due to periodic variations of the order parameter $\epsilon_{ij}(\vec{r})$. We therefore set $\tilde{\epsilon}=0$ in (17b). It follows that $\tilde{\mu}_{34}=\tilde{\mu}_{43}=0$.

(a) Backscattering configurations; $\theta=\pi/2$. Here we are necessarily interested in the *total* scattered intensity matrix $\underline{\Phi}_T=4\pi rcs\underline{\Phi}$. The reduced matrix $\underline{\tilde{\mu}}$ takes the form

$$(\underline{\tilde{\mu}})_{\theta=\pi/2}=\begin{pmatrix} \frac{4}{3}\epsilon_0^2+4(\epsilon_2^2+\epsilon_{-2}^2) & 0 & 0 & -4(\epsilon_2^2-\epsilon_{-2}^2) \\ 0 & \frac{4}{3}\epsilon_0^2 & 0 & 0 \\ 0 & 0 & -\frac{4}{3}\epsilon_0^2 & 0 \\ -4(\epsilon_2^2-\epsilon_{-2}^2) & 0 & 0 & -\frac{4}{3}\epsilon_0^2 \end{pmatrix} . \tag{25}$$

Note that $m=\pm1$ elements of $\underline{\epsilon}(\sigma)$ are unobservable in this configuration.

(b) $\theta\neq\pi/2$. In the usual cholesteric phase there is only one Bragg peak, associated with either ϵ_2 or ϵ_{-2}, depending upon whether the helix is left- or right-handed. From the Landau theory of blue phases[13(h)] it follows that here also a single amplitude, again either ϵ_2 or ϵ_{-2}, will be the dominant contribution to each Bragg peak (except, of course, where this amplitude vanishes by symmetry,[13(d),13(h)] in which case the corresponding Bragg peak is expected to be weak). When only this dominant contribution is considered, the reduced matrix has the form

$$\underline{\tilde{\mu}}=\epsilon_{\pm2}^2\begin{pmatrix} (s^2+1)^2 & -(1-s^4) & 0 & \mp2s(s^2+1) \\ -(1-s^4) & c^4 & 0 & \pm2sc^2 \\ 0 & 0 & 0 & 0 \\ \mp2s(s^2+1) & \pm2sc^2 & 0 & 4s^2 \end{pmatrix} . \tag{26a}$$

In particular, for $\theta=\pi/4$, which has been recently studied by Flack *et al.*,[3(d)] (26a) becomes

$$(\underline{\tilde{\mu}})_{\theta=\pi/4}=\tfrac{9}{4}\epsilon_{\pm2}^2\begin{pmatrix} 1 & -\frac{1}{3} & 0 & \mp2\sqrt{2}/3 \\ -\frac{1}{3} & \frac{1}{9} & 0 & \pm\sqrt{2}/9 \\ 0 & 0 & 0 & 0 \\ \mp2\sqrt{2}/3 & \pm\sqrt{2}/9 & 0 & \frac{8}{9} \end{pmatrix} . \tag{26b}$$

For comparison with the experimental results, it is necessary to modify (26b) since Flack *et al.*[3(d)] used a coordinate frame in which x rather than y was taken to be perpendicular to the scattering plane. For this frame the modified matrix $\tilde{\mu}'$ can be obtained from (17b) by reversing the algebraic signs of elements $\tilde{\mu}_{ij}$ having $(i+j)$ odd ($\tilde{\mu}_{12},\tilde{\mu}_{14},\tilde{\mu}_{21},\tilde{\mu}_{23},\tilde{\mu}_{32},\tilde{\mu}_{34},\tilde{\mu}_{41},\tilde{\mu}_{43}$). In particular, (26b) becomes

$$(\underline{\tilde{\mu}}')_{\theta=\pi/4}=\frac{9}{4}\epsilon_{\pm 2}^2\begin{bmatrix} 1 & \frac{1}{3} & 0 & \pm 2\sqrt{2}/3 \\ \frac{1}{3} & \frac{1}{9} & 0 & \pm\sqrt{2}/9 \\ 0 & 0 & 0 & 0 \\ \pm 2\sqrt{2}/3 & \pm\sqrt{2}/9 & 0 & \frac{8}{9} \end{bmatrix} . \tag{26c}$$

The normalized matrix in (26c) with $\epsilon_2 \neq 0$ is in suprisingly good agreement with the experimental results, the main discrepancy arising from the observation of small, but nonvanishing contributions to the elements $\tilde{\mu}_{i3}, \tilde{\mu}_{3i}$. This point will be explored further in Sec. II C, where the role of optical activity is analyzed.

(c) Weak contributions (ϵ_1). An efficient way of distinguishing among alternate space group assignments for BP would be to detect, in addition to the dominant ϵ_2 or ϵ_{-2} contribution to a particular reflection, the presence of other components of $\underline{\epsilon}(\sigma)$. When, for example, ϵ_2 is the lowest-lying state, one would like to determine whether the next-lowest-lying state, ϵ_1, is occupied or not. Let us therefore consider $\underline{\tilde{\mu}}$ for the case in which only ϵ_2 and $\epsilon_1 \neq 0$. We obtain

$$\underline{\tilde{\mu}}=\begin{bmatrix} \epsilon_2^2(s^2+1)^2+2\epsilon_1^2c^2 & -\epsilon_2^2(1-s^4) & 0 & -2\epsilon_2^2s(s^2+1) \\ -\epsilon_2^2(1-s^4) & \epsilon_2^2c^4-2\epsilon_1^2c^2 & 0 & 2\epsilon_2^2sc^2 \\ 0 & 0 & 2\epsilon_1^2c^2 & 0 \\ -2\epsilon_2^2s(s^2+1) & 2\epsilon_2^2sc^2 & 0 & 4\epsilon_2^2s^2-2\epsilon_1^2c^2 \end{bmatrix} . \tag{27}$$

From (27), we see that in order to detect the presence of an ϵ_1 component, the best approach is to make θ as small as experimentally possible (this will be fixed in most cases by the shortest obtainable wavelength of the light source) and to measure $\tilde{\mu}_{33}$. For example, at $\theta=\pi/6$, we have, from (27),

$$\mu_{33}/\mu_{11} \approx \tfrac{24}{25}(\epsilon_1^2/\epsilon_2^2), \quad \epsilon_1^2 \ll \epsilon_2^2 . \tag{28}$$

With a system capable of measuring matrix element ratios of 1—4%, (28) indicates that ϵ_1/ϵ_2 ratios of 0.1—0.2 would be detectable. This might be sufficient to distinguish between, on the one hand, the bcc space groups T^3 ($I23$) and T^5 ($I2_13$) and, on the other hand, bcc O^8 ($I4_132$) and sc O^2 ($P4_232$) and T^1 ($P23$) (see Table I). For the former, an ϵ_1 component is *allowed* in the primary Bragg reflection while in the latter it is *forbidden*. Of course, the nondetection of ϵ_1 can never be conclusive, since its magnitude could be nonzero but nevertheless below the sensitivity of the detection system.

(d) Weak contributions (ϵ_0). In order to distinguish between the two most commonly proposed structures,[13(h)] bcc O^8 and sc O^2, a search for an ϵ_1 contribution to the scattered Stokes vector will not be useful since, by symmetry, $\epsilon_1=0$ for both the first and second Bragg reflections in either of these structures, as noted in Table I. It becomes necessary, therefore, to search for an ϵ_0 component in $\epsilon_{ij}(\sigma)$. For the case in which only $\epsilon_2, \epsilon_0 \neq 0$, $\underline{\tilde{\mu}}$ becomes

$$\underline{\tilde{\mu}}=\begin{bmatrix} \frac{2}{3}\epsilon_0^2[(c^2+1)^2+1]+\epsilon_2^2(s^2+1)^2 & \frac{2}{3}\epsilon_0^2[(c^2+1)^2-1] & 0 & -2\epsilon_2^2s(s^2+1) \\ \frac{2}{3}\epsilon_0^2[(c^2+1)^2-1] & \frac{2}{3}\epsilon_0^2[(c^2+1)^2+1]+\epsilon_2^2c^4 & 0 & 2\epsilon_2^2sc^2 \\ 0 & 0 & \frac{4}{3}\epsilon_0^2(c^2+1) & 0 \\ -2\epsilon_2^2s(s^2+1) & 2\epsilon_2^2sc^2 & 0 & \frac{4}{3}\epsilon_0^2(c^2+1)+4\epsilon_2^2s^2 \end{bmatrix} . \tag{29}$$

TABLE I. Optical structure factor for chiral cubic space groups. $S(W)$ denotes a strong (weak) Bragg reflection. X-ray selection rules are identical to those for $m=0$.

		Body-centered cubic			
		T^3	T^5	O^5	O^8
		$h+k+l=2n$ $h00{:}m=\pm2,0$ $hhh{:}\,m=0$	$h+k+l=2n$ $h00{:}m=\pm2,0$ $hhh{:}\,m=0$	$h+k+l=2n$ $h00{:}m=0$ $hh0{:}m=\pm2,0$ $hhh{:}\,m=0$	$h+k+l=2n$ $h00{:}m=\pm2;h=4n-2$ $m=0;h=4n$ $hh0{:}\,m=\pm2,0$ $hhh{:}\,m=0$
$\frac{1}{2}(h^2+k^2+l^2)$	hkl	m			
		2 1 0 −1−2	2 1 0 −1−2	2 1 0 −1−2	2 1 0 −1−2
1	110	+++ + + S	+++ + + S	+−+ − + S	+−+ − + S
2	200	+−+ − + S	+−+ − + S	−−+ − − W_0	+−− − + S
3	211	+++ + + S	+++ + + S	+++ + + S	+++ + + S
4	220	+++ + + S	+++ + + S	+−+ − + S	+−+ − + S
5	310	+++ + + S	+++ + + S	+++ + + S	+++ + + S
6	222	−−+ − − W_0	−−+ − − W_0	−−+ − − W_0	−−+ − − W_0
7	321	+++ + + S	+++ + + S	+++ + + S	+++ + + S
8					
9	330	+++ + + S	+++ + + S	+−+ − + S	+−+ − + S

		Simple cubic					
		T^1	T^4	O^1	O^2	O^6	O^7
		$h00{:}m=\pm2,0$ $hhh{:}\,m=0$	$h00{:}m=\pm1;h=2n-1$ $m=\pm2,0;h=2n$ $hhh{:}\,m=0$	$h00{:}m=0$ $hh0{:}m=\pm2,0$ $hhh{:}\,m=0$	$h00{:}m=\pm2;h=2n-1$ $m=0;h=2n$ $hh0{:}m=\pm2,0$ $hhh{:}\,m=0$	$h00{:}m=\pm1;h=4n-3$ $m=\pm2;h=4n-2$ $m=-1;h=4n-1$ $m=0;h=4n$ $hh0{:}m=\pm2,0$ $hhh{:}\,m=0$	$h00{:}m=-1;h=4n-3$ $m=\pm2;h=4n-2$ $m=1;h=4n-1$ $m=0;h=4n$ $hh0{:}m=\pm2,0$ $hhh{:}\,m=0$
$h^2+k^2+l^2$	hkl	m					
		2 1 0 −1−2	2 1 0 −1−2	2 1 0 −1−2	2 1 0 −1 −2	2 1 0 −1−2	2 1 0−1−2
1	100	+−+ − + S	−+− + − W_1	−−+ − − W_0	+−− − + S	−+− − − W_1	−−− + − W_1
2	110	+++ + + S	+++ + + S	+−+ − + S	+−+ − + S	+−+ − + S	+−+ − + S
3	111	−−+ − − W_0	−−+ − − W_0	−−+ − − W_0	−−+ − − W_0	−−+ − − W_0	−−+ − − W_0
4	200	+−+ − + S	+−+ − + S	−−+ − − W_0	−−+ − − W_0	+−− − + S	+−− − + S
5	210	+++ + + S	+++ + + S	+++ + + S	+++ + + S	+++ + + S	++± + + S
6	211	+++ + + S	+++ + + S	+++ + + S	+++ + + S	+++ + + S	+++ + + S
7							
8	220	+++ + + S	+++ + + S	+−+ − + S	+−+ − + S	+−+ − + S	+−+ − + S
9	221	+++ + + S	+++ + + S	+++ + + S	+++ + + S	+++ + + S	+++ + + S

As in the previous case, it is again desirable to make θ as small as possible and to attempt to detect μ_{33}. For $\theta=\pi/6$, for example, we have

$$\mu_{33}/\mu_{11}\approx\tfrac{112}{75}(\epsilon_0^2/\epsilon_2^2),\quad \epsilon_0^2\ll\epsilon_2^2\ . \tag{30}$$

With an experimental detection ratio sensitivity of 1—4%, ϵ_0/ϵ_2 ratios of 0.08—0.16 would be detectable. Finding $\epsilon_0\neq 0$ for the primary reflection would rule out an O^2 structure while a positive result for the second Bragg peak would rule out O^8.

(e) Transmission. Rather than measuring scattered Bragg intensities, it is possible to study the nonscattered or transmitted intensity as a function of the wavelength λ of the incident beam. Experiments of this type have been carried out by Meiboom and Sammon.[2] In this configuration, there is a series of steps (reductions) in the transmitted intensity with decreasing λ, with each step occurring when the Bragg condition for backscattering at a given (hkl) is satisfied. From (17), (18), and (24), we find that the tensor $\Delta\underline{\Phi}_T$ associated with each step is given by

$$\Delta\underline{\Phi}_T(\sigma)=4\pi rcs(\underline{\Phi})_{\theta=\pi/2}$$
$$=(\pi^2N^2V/32n^4\lambda_\sigma)(\underline{\tilde{\mu}})_{\theta=\pi/2}\underline{I}\ , \tag{31}$$

where

$$\lambda_\sigma=4\pi/Q=4\pi/q\sigma^{1/2}\ .$$

When total intensity is being measured, we have

$$[\Delta\underline{\Phi}_T(\sigma)]_1=(\pi^2N^2V/8n^4\lambda_\sigma)$$
$$\times[(\epsilon_2^2+\epsilon_{-2}^2)+\tfrac{1}{3}\epsilon_0^2]I_1\ , \tag{32a}$$

or, when only the dominant ϵ_2 contribution is considered,

$$[\Delta\underline{\Phi}_T(\sigma)]_1=(\pi^2N^2V/8n^4\lambda_\sigma)\epsilon_2^2I_1\ . \tag{32b}$$

In the region $\lambda<\lambda_\sigma$, but before the following Bragg reflection threshold is reached, the total *scattered* intensity in the presence of the $\sigma'\leq\sigma$ Bragg reflections becomes

$$[\underline{\Phi}_T(\lambda)]_1=\tfrac{1}{4}\sum_{\sigma'\leq\sigma}[\Delta\underline{\Phi}_T(\sigma')]_1\left[\frac{\lambda}{\lambda_{\sigma'}}+\frac{\lambda_{\sigma'}}{\lambda}\right]^2 \tag{33}$$

when only $\epsilon_2(\sigma')\neq 0$. [If $\epsilon_2(\sigma')=0$ for particular values of σ' (see Table I), these σ' values do not contribute to the sum in (33).] A comparison between (33) and the experimental results of Meiboom and Sammon[2(b)] is shown in Fig. 2.

Another experimentally accessible quantity is the ratio of right-hand (rh) to left-hand (lh) polarized scattered light. For example, between the first and second Bragg reflections this ratio is given by

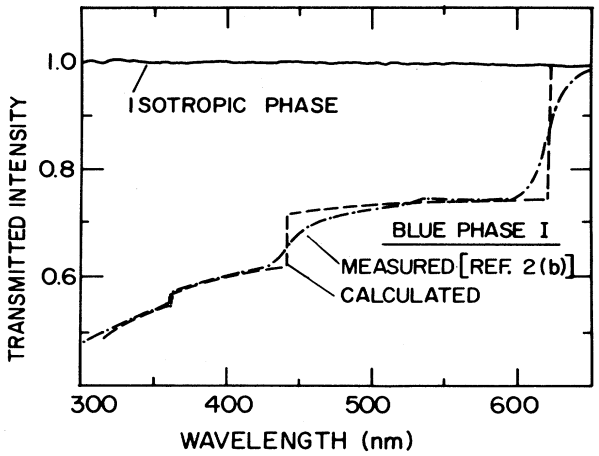

FIG. 2. Comparison of the transmitted intensity calculated theoretically using Eq. (33) with the experimental results of Meiboom and Sammon, Ref. 2(b). The steps (but *not* the relative positions) at each of the three Bragg reflections were fitted to the reported data.

$$\frac{\Phi_T(\mathrm{rh};\lambda)}{\Phi_T(\mathrm{lh};\lambda)}=\left|\frac{\tilde{\mu}_{11}+\tilde{\mu}_{14}}{\tilde{\mu}_{11}-\tilde{\mu}_{14}}\right|=\frac{(\lambda_1/\lambda)^2-1}{(\lambda_1/\lambda)^2+1}\ ,$$
$$1\leq\lambda_1/\lambda<\sqrt{2}\ . \tag{34}$$

C. The effect of optical activity

In Sec. II B we derived, using the Mueller matrix approach, the matrix describing the elastic Bragg scattering of an ordered polycrystalline cholesteric liquid-crystal system in the weak scattering limit. This was done by calculating the linear relation between the Stokes vectors characterizing the light beam before and after the scattering event. In an actual experiment, however, the light beam will in general pass through a length l_α of the sample before the scattering event and, similarly, a length l_β following it. Since the blue phases exhibit significant optical activity, it is clear that the Stokes vector of the incoming light beam will be modified before the Bragg reflection takes place while the measured outgoing beam Stokes vector will differ from that existing immediately following the reflection. In this section we calculate the appropriate Mueller matrix to describe this process. This is essentially equivalent to taking into account the effect of weak multiple reflections.

We begin by noting that in the Mueller matrix formalism the modified matrix $\underline{\mu}_t$ is defined as in (18) by

$$\underline{\Phi}=\underline{\mu}_t\underline{I}=\tfrac{1}{8}\tilde{g}^2\underline{\tilde{\mu}}_t\underline{I}=\tfrac{1}{8}\tilde{g}^2\underline{\mu}_\beta\underline{\tilde{\mu}}\underline{\mu}_\alpha\underline{I}\ , \tag{35}$$

where $\underline{\mu}_\alpha, \underline{\mu}_\beta$ are the matrices describing the effect of optical activity before and after the scattering event, respectively. Specifically, both these matrices, for *given* l_α, l_β, have the form

$$\underline{\mu}_i = \begin{vmatrix} 1 & 0 & 0 & 0 \\ 0 & \tilde{c}_i & \tilde{s}_i & 0 \\ 0 & -\tilde{s}_i & \tilde{c}_i & 0 \\ 0 & 0 & 0 & 1 \end{vmatrix}, \quad i=\alpha,\beta \tag{36}$$

where

$$\tilde{c}_i = \cos(2\delta l_i) ,$$

and

$$\tilde{s}_i = \sin(2\delta l_i) ,$$

and δ is the optical activity coefficient (in radians per unit length). This quantity has been recently calculated for the BP.[19] Since in most experimental configurations $l_\alpha = l_\beta$, we restrict ourselves to this case. From (17) (with $\tilde{\epsilon}=0$), (35), and (36), we obtain

$$\underline{\tilde{\mu}}_t = \begin{vmatrix} \tilde{\mu}_{11} & \tilde{\mu}_{12}\bar{c} & \tilde{\mu}_{12}\bar{s} & \tilde{\mu}_{14} \\ \tilde{\mu}_{12}\bar{c} & \tilde{\mu}_{22}\overline{c^2}-\tilde{\mu}_{33}\overline{s^2} & (\tilde{\mu}_{22}+\tilde{\mu}_{33})\overline{sc} & \tilde{\mu}_{24}\bar{c} \\ -\tilde{\mu}_{12}\bar{s} & -(\tilde{\mu}_{22}+\tilde{\mu}_{33})\overline{sc} & -\tilde{\mu}_{22}\overline{s^2}+\tilde{\mu}_{33}\overline{c^2} & -\tilde{\mu}_{24}\bar{s} \\ \tilde{\mu}_{14} & \tilde{\mu}_{24}\bar{c} & \tilde{\mu}_{24}\bar{s} & \tilde{\mu}_{44} \end{vmatrix} . \tag{37}$$

Here we have dropped the index i in (36) and the bar denotes the average value of the quantity. From (37) and noting that $l_\alpha = l_\beta$ takes on with equal weight all values between zero and a maximum l_0 proportional to the specimen thickness and the scattering angle, we have

$$\begin{aligned} (\mu_t)_{13}/(\mu_t)_{12} &= (\mu_t)_{43}/(\mu_t)_{42} = \bar{s}/\bar{c} \\ &= \tan(2\delta l_0) , \\ 2(\mu_t)_{23}/[(\mu_t)_{22}+(\mu_t)_{33}] &= 2\overline{sc}/(\overline{c^2}-\overline{s^2}) \\ &= \tan(2\delta l_0) . \end{aligned} \tag{38}$$

Thus these ratios allow us to determine the optical activity contribution to $\underline{\tilde{\mu}}_t$. Note that (37) gives, for $\delta l_0 \ll 1$, $O(l_0^2)$ corrections to the scattering cross section.

We now consider the effect of optical activity in the experimental configurations discussed in Sec. II B.

(a) Backscattering configuration: $\theta=\pi/2$. Using (25), we obtain

$$(\underline{\tilde{\mu}}_t)_{\theta=\pi/2} = \begin{vmatrix} \frac{4}{3}\epsilon_0^2+4(\epsilon_2^2+\epsilon_2^2) & 0 & 0 & -4(\epsilon_2^2-\epsilon_{-2}^2) \\ 0 & \frac{4}{3}\epsilon_0^2(\overline{c^2}+\overline{s^2}) & 0 & 0 \\ 0 & 0 & -\frac{4}{3}\epsilon_0^2(\overline{c^2}+\overline{s^2}) & 0 \\ -4(\epsilon_2^2-\epsilon_{-2}^2) & 0 & 0 & -\frac{4}{3}\epsilon_0^2 \end{vmatrix} . \tag{39}$$

In this configuration, we see that optical activity has essentially no effect on the observed Stokes vector.

(b) $\theta=\pi/4$ scattering configuration. For a $\theta=\pi/4$ scattering configuration and a $\underline{\tilde{\mu}}$ matrix in which only $\epsilon_2 \neq 0$, (37) becomes [in the coordinate frame of Flack *et al.*,[3(d)] defined earlier and used in (26c)]

$$(\underline{\tilde{\mu}}_t')_{\theta=\pi/4} = \frac{9}{4}\epsilon_2^2 \begin{vmatrix} 1 & \bar{c}/3 & \bar{s}/3 & 2\sqrt{2}/3 \\ \bar{c}/3 & \overline{c^2}/9 & \overline{sc}/9 & c\sqrt{2}/9 \\ -\bar{s}/3 & -\overline{sc}/9 & -\overline{s^2}/9 & -s\sqrt{2}/9 \\ 2\sqrt{2}/3 & \bar{c}\sqrt{2}/9 & \bar{s}\sqrt{2}/9 & \frac{8}{9} \end{vmatrix} . \tag{40}$$

Whenever $2\delta l_0 \ll 1$ (i.e., weak optical activity or thin sample), we see from (37) and (40) that the main consequence of optical activity [for $\tilde{\mu}_{12}$ and $(\tilde{\mu}_{22}+\tilde{\mu}_{33}) \neq 0$)] is the nonvanishing of the matrix elements $(\tilde{\mu}_t)_{13}$, $(\tilde{\mu}_t)_{23}$, and $(\tilde{\mu}_t)_{43}$ [and their transposes, which are given by $(\tilde{\mu}_t)_{3i} = -(\tilde{\mu}_t)_{i3}$, $i \neq 3$].

These elements are all proportional to $\bar{s}\simeq\delta l_0$. Interestingly, $(\tilde{\mu}_t)_{33}$, which is proportional to s^2 when $\tilde{\mu}_{33}=0$, is essentially unaffected by the optical activity in this limit.

The normalized matrix in (40), with $\bar{s}\simeq\frac{1}{3}$, $\bar{c}\simeq 1$, is in excellent agreement with the measured Mueller matrix[3(d)] characterizing the first and second Bragg reflections for both BPI and BPII. In this particular experiment, contributions from components of $\underline{\epsilon}(\sigma)$ other than ϵ_2 are clearly either small or nonexistent (less than 4%, according to Flack *et al.*[3(d)]). Thus scattering experiments of the type described here whose goal is to detect such contributions require sensitive measuring techniques. However, since our analysis shows that optical activity results essentially in contributions to Mueller matrix elements which would otherwise vanish, it does not make the experimental task of detecting these small contributions more difficult than it would be otherwise.

D. Bragg scattering by single crystals

In Sec. II B we derived the Mueller matrix characterizing Bragg scattering by a polycrystalline periodically ordered liquid crystal specimen. As discussed earlier, one would like to use these results to distinguish between different periodically ordered structures and this, in general, requires detection of ϵ_1 and ϵ_0 components of the order parameter amplitude tensor $\underline{\epsilon}(\sigma)$ associated with a particular Bragg peak. These components are expected to be weak relative to the dominant ϵ_2 (we assume, for definiteness, a left-handed cholesteric spiral structure) component and, for a polycrystalline specimen, enter quadratically into the Mueller matrix. Thus detection of these components presents difficulties.

One possible way of circumventing this would be to study Bragg scattering by a single crystal, rather than by a polycrystalline specimen. This, of course, requires that such specimens be available. The recent results of Onusseit and Stegemeyer[11] and Marcus[7(b)] indicate, however, that such specimens can definitely be grown in BPII and possibly also in BPI. Thus single-crystal light-scattering studies could be a promising approach. In this section we shall derive the Mueller matrix characterizing such scattering. We again assume that the scattering is weak, ignoring extinctions and similar difficulties. It must be stressed, however, that such effects can be much more serious in single crystal than in polycrystalline scattering studies.

In order to simplify our algebraic expressions while preserving the essential elements of the calculation, we shall (a) neglect *ab initio* any contributions from the density variation $\tilde{\epsilon}$ and higher-lying components ϵ_{-1} and ϵ_{-2}, and (b) keep only terms of order ϵ_2^2, $\epsilon_2\epsilon_1$, and $\epsilon_2\epsilon_0$. Returning to (9), we have, therefore,

$$\begin{aligned} E_{\beta 1}&=\tfrac{1}{2}g\{[-\epsilon_2\alpha_2 s^2+\epsilon_0\alpha_0(1+c^2)]E_{\alpha 1} \\ &\quad +i(\epsilon_2\alpha_2+\epsilon_1\alpha_1)E_{\alpha 2}\}\ , \\ E_{\beta 2}&=\tfrac{1}{2}g[-i(\epsilon_2\alpha_2 s-\epsilon_1\alpha_1 c)E_{\alpha 1} \\ &\quad -(\epsilon_2\alpha_2+\epsilon_0\alpha_0)E_{\alpha 2}]\ . \end{aligned} \tag{41}$$

Instead of (10a) the outgoing beam Jones matrix is

$$\underline{J}_\beta=\begin{bmatrix}\sum E_{\beta 1}E^*_{\beta 1}\\ \sum E_{\beta 1}E^*_{\beta 2}\\ \sum E^*_{\beta 2}E_{\beta 1}\\ \sum E_{\beta 2}E^*_{\beta 2}\end{bmatrix}=\underline{T}\,\underline{J}_\alpha\ . \tag{42}$$

The elements of $\underline{T}$, from (10b), (41), and (42), are

$$\begin{aligned} T_{11}&=\epsilon_2^2 s^4-\epsilon_2\epsilon_0 s^2(1+c^2)(\alpha_2\alpha_0^*+\alpha_2^*\alpha_0)\ , \\ T_{12}&=T_{13}^*=i\epsilon_2^2 s^3+i\epsilon_2\epsilon_1 s^2 c\alpha_2\alpha_1^* \\ &\quad -i\epsilon_2\epsilon_0 s(1+c^2)\alpha_2^*\alpha_0\ , \\ T_{14},T_{41}&=\epsilon_2^2 s^2\pm\epsilon_2\epsilon_1 sc(\alpha_2\alpha_1^*+\alpha_2^*\alpha_1)\ , \\ T_{21}&=T_{31}^*=-i\epsilon_2^2 s^3+i\epsilon_2\epsilon_1 s^2 c\alpha_2\alpha_1^* \\ &\quad +i\epsilon_2\epsilon_0 s(1+c^2)\alpha_2^*\alpha_0\ , \\ T_{22}&=T_{33}^*=\epsilon_2^2 s^2+\epsilon_2\epsilon_0[s^2\alpha_2\alpha_0^*-(1+c^2)\alpha_2^*\alpha_0]\ , \\ T_{23}&=T_{32}^*=-\epsilon_2^2 s^2-\epsilon_2\epsilon_1 sc(\alpha_2\alpha_1^*-\alpha_2^*\alpha_1)\ , \\ T_{24}&=T_{34}^*=-i\epsilon_2^2 s-i\epsilon_2\epsilon_1 c\alpha_2^*\alpha_1-i\epsilon_2\epsilon_0 s\alpha_2\alpha_0^*\ , \\ T_{42}&=T_{43}^*=i\epsilon_2^2 s+i\epsilon_2\epsilon_1 c\alpha_2^*\alpha_1+i\epsilon_2\epsilon_0 s\alpha_2\alpha_0^*\ , \\ T_{44}&=\epsilon_2^2+\epsilon_2\epsilon_0(\alpha_2\alpha_0^*+\alpha_2^*\alpha_0)\ . \end{aligned} \tag{43}$$

Note that in the single crystal case $\underline{T}$ is not Hermitian. From (12), (15), (16), and (43), and following the definition in (18), we obtain the Mueller matrix $\underline{\mu}_c$ for single-crystal scattering as

$$\underline{\Phi}=\underline{\mu}_c\underline{I}=\tfrac{1}{8}\tilde{g}^2\underline{\bar{\mu}}\,\underline{I}\ , \tag{44a}$$

with

$$\begin{aligned} \bar{\mu}_{11}&=\epsilon_2^2(s^2+1)^2+c^4C_{20}\ , \\ \bar{\mu}_{12},\bar{\mu}_{21}&=-\epsilon_2^2(1-s^4)\mp s_2C_{21}\ -(2-c^4)C_{20}\ , \\ \bar{\mu}_{13},\bar{\mu}_{31}&=\pm c(1\mp s^2)S_{21}-s(2+c^2)S_{20}\ , \\ \bar{\mu}_{14},\bar{\mu}_{41}&=-2\epsilon_2^2 s(s^2+1)-c(1\pm s^2)C_{21}+sc^2C_{20}\ , \\ \bar{\mu}_{22}&=\epsilon_2^2 c^4+c^4C_{20}\ , \end{aligned} \tag{44b}$$

$$\bar{\mu}_{23},\bar{\mu}_{32}=\mp c(1\pm s^2)S_{21}-sc^2S_{20}\ ,$$
$$\bar{\mu}_{24},\bar{\mu}_{42}=2\epsilon_2^2sc^2+c(1\mp s^2)C_{21}+s(2+c^2)C_{20}\ ,$$
$$\bar{\mu}_{33}=-2c^2C_{20}\ ,$$
$$\bar{\mu}_{34},\bar{\mu}_{43}=s_2S_{21}\mp 2S_{20}\ ,$$
$$\bar{\mu}_{44}=4\epsilon_2^2s^2-2c^2C_{20}\ ,$$

and

$$\begin{aligned} C_{21}&=2\epsilon_2\epsilon_1\cos(\psi_2-\psi_1)\ ,\\ S_{21}&=2\epsilon_2\epsilon_1\sin(\psi_2-\psi_1)\ ,\\ C_{20}&=2\sqrt{2/3}\epsilon_2\epsilon_0\cos(\psi_2-\psi_0)\ ,\\ S_{21}&=2\sqrt{2/3}\epsilon_2\epsilon_0\sin(\psi_2-\psi_0)\ . \end{aligned} \tag{44c}$$

We now consider some specific crystallographic structures. Recently, Onusseit and Stegemeyer[11(a)] and Marcus[7(b)] found that in BPII single crystals can be grown in the form of large square platelets and also that the primary Bragg reflection is observed normal to the platelets by backscattering. On morphological grounds Marcus[7(b)] has argued that the platelet edges are parallel to ⟨100⟩ crystallographic directions and that the BPII structure is sc. This conclusion is supported by the work of Flack and Crooker,[3(b)] who could not detect the third Bragg reflection in the phase they called BPIIA, but which has since been argued[7(e)] to be BPII. This particular reflection can be due only to ϵ_0 in sc structures[13(d),(h)] and will be, at best, extremely weak for a polycrystalline specimen. If it is therefore accepted that BPII is sc, it follows that this phase should be assigned to either the O^2 or T^1 space group. One way[13(d),13(h)] of distinguishing between these two possibilities (see Table I) is to note that for the primary (100) reflection an ϵ_0 component is *forbidden* in the case of O^2, but *allowed* in the case of T^1. For a *backscattering configuration,* (44) becomes

$$\underline{\bar{\mu}}=\begin{bmatrix} 4\epsilon_2^2 & -2C_{20} & -2S_{20} & -4\epsilon_2^2 \\ -2C_{20} & 0 & 0 & 2C_{20} \\ -2S_{20} & 0 & 0 & 2S_{20} \\ -4\epsilon_2^2 & 2C_{20} & -2S_{20} & 4\epsilon_2^2 \end{bmatrix}. \tag{45}$$

For the O^2 (100) reflection, $C_{20}=S_{20}=0$, and only the elements

$$\bar{\mu}_{11}=\bar{\mu}_{44}=-\bar{\mu}_{14}=-\bar{\mu}_{41}$$

are nonzero. [Remember that the terms of $O(\epsilon_{-2}^2)$ which appeared in (25) are here neglected.] For T_1, on the other hand, additional elements of $\underline{\bar{\mu}}$ can be nonzero. For this case, the phases ψ_2 and ψ_0 are either 0 or π for all ⟨100⟩, thus the effect of $\epsilon_0\neq 0$ will be reflected in the elements

$$\bar{\mu}_{12}=\bar{\mu}_{21}=-\bar{\mu}_{24}=-\bar{\mu}_{42}=0\ .$$

The ratio

$$|\bar{\mu}_{12}/\bar{\mu}_{11}|=|C_{20}/2\epsilon_2^2|=(\tfrac{2}{3})^{1/2}\epsilon_0/\epsilon_2\ , \tag{46}$$

should be observable even if ϵ_0 is only a few percent of ϵ_2.

While detecting an $\epsilon_0\neq 0$ contribution to $\underline{\bar{\mu}}$ would eliminate O^2, a null result cannot, as noted previously, be regarded as definite. One should also search for an ϵ_0 contribution to the second Bragg peak which, for an sc structure, would be the (110) reflection. To observe it in a backscattering configuration, it is necessary to orient the incident beam at a $\pi/4$ angle to the platelet normal, and also perpendicular to one of the platelet edges. Again, all ψ_2 and ψ_0 are either 0 or π for both sc space groups. Thus the appropriate Mueller matrix is (45) with $S_{20}=0$. Finding (see Table I) $\epsilon_0(\sigma=1)=0$ and $\epsilon_0(\sigma=2)\neq 0$ would provide strong support for an O^2 structure assignment while finding both $\epsilon_0(\sigma=1)$, $\epsilon_0(\sigma=2)\neq 0$ would point to a T^1 structure. Of course, it would also be useful to confirm that BPII is sc by searching for the weak third reflection. In backscattering, a (111) reflection should be searched for by orienting the incident beam along a [111] crystallographic direction. For an sc lattice, the appropriate Mueller matrix is (25), with only $\epsilon_0\neq 0$. For all bcc lattices there will be, on the other hand, the strong ϵ_2 contributions appearing in (45).

We now consider BPI. Oriented BPI platelets have been obtained by first creating platelets in BPII and then lowering the temperature.[7(b),11(a)] These platelets are apparently not single crystals, but rather sets of strongly oriented polycrystals. Since, however, each set satisfies the Bragg condition separately, we can regard these platelets as being essentially single crystals. Based on morphological considerations and his observation of the primary Bragg reflection in backscattering along a direction perpendicular to the plane of the platelet, Marcus[7(b)] has argued that BPI is bcc with a [110] crystallographic direction along the platelet normal. The possible bcc space group assignments are O^8, its subgroup T^5, and T^3. Landau theory calculations[13(h)] indicate that the latter is relatively unlikely. Note that the results of Flack and Crooker[3(b)] and also those of

Meiboom and Sammon[2] definitely eliminate any sc group assignment as well (at least for the materials studied by them) as well as the other possible bcc space group, O^5 ($I432$).

While one cannot distinguish between T^5 and T^3 by Mueller matrix studies,[13(d),13(h)] it is possible in principle to determine whether the structure belongs to one of these groups or to O^8. The best way of doing this is to utilize the structure factor information[13(d),13(h)] for the two Bragg peaks, (110) and (200). From Table I, it is clear that we should search for a $\epsilon_1(2)$ component in the first Bragg peak and an $\epsilon_0(4)$ component in the second. Their presence would rule out an O^8 structure assignment and vice versa for T^3 or T^5. The search for an $\epsilon_2(2)$ contribution is, however, complicated by the presence of an $\epsilon_0(2)$ component for all structures. Also, as noted earlier, ϵ_1 contributions cannot be detected in a backscattering configuration and, for each such contribution, either C_{21} or S_{21} (but not both) will be identically zero.

III. THE MUELLER MATRIX FORMALISM; SCATTERING IN THE ISOTROPIC PHASE

A. Thermal fluctuations

In the disordered or isotropic phase, the average value of all $q\neq 0$ components of ϵ_{ij}^d is, of course, zero. Owing, however, to thermal fluctuations, the *squares* of these quantities are nonvanishing and, to lowest order, can be simply calculated using the equipartition theorem.

For cholesteric systems, the average free-energy density is given by[24,25]

$$F=V^{-1}\int d\vec{r}\,[\tfrac{1}{2}(a\epsilon_{ij}^2+c_1\epsilon_{ij,l}^2+c_2\epsilon_{ij,i}\epsilon_{lj,l}-2de_{ijl}\epsilon_{in}\epsilon_{jn,l})-\beta\epsilon_{ij}\epsilon_{jl}\epsilon_{li}+\gamma(\epsilon_{ij}^2)^2]\ , \tag{47}$$

where, as usual, a is proportional to a reduced temperature, c_1, c_2, d, β, and γ are regarded as temperature-independent parameters,

$$\epsilon_{ij,l}\equiv\partial\epsilon_{ij}/\partial x_l\ ,$$

and we sum on repeated indices. From thermodynamic considerations it is necessary that c_1 and γ be positive and that [13(h)] $c_1+\frac{2}{3}c_2>0$.

We restrict ourselves here to the *harmonic approximation,* in which the fluctuation-induced contributions to the free energy are given by the quadratic (order ϵ^2) terms in (47). However, it should be noted that contributions from the higher-order terms may be important close to the clearing point.[13(g)] We again expand $\epsilon_{ij}(\vec{r};\omega)$ in Fourier components, replacing

$$q(h\hat{i}_x+k\hat{i}_y+l\hat{i}_z)$$

in (2) by $\vec{Q}$ and noting that now the multiplicity N is 1. We then have

$$\epsilon_{ij}(\vec{r})=\sum_{\vec{Q}}\epsilon_{ij}(Q)\exp(i\vec{Q}\cdot\vec{r})\ . \tag{48}$$

Substituting (48) into the quadratic part of (47) and using (2b), we obtain

$$F_2=\tfrac{1}{2}\sum_{\vec{Q},m}\{a-mdQ+[c_1+\tfrac{1}{6}c_2(4-m^2)]Q^2\}\times\epsilon_m^2(Q)\ . \tag{49}$$

From the equipartition theorem, we have

$$\langle\epsilon_m(Q)\epsilon_{m'}(-Q')\rangle=\delta_{mm'}\delta_{\vec{Q}\,\vec{Q}'}\frac{k_BT/V}{a-mDQ+[c_1+\frac{1}{6}c_2(4-m^2)]Q^2}\ , \tag{50a}$$

where k_B is Boltzmann's constant and T is the temperature. The brackets denote a thermodynamic average. In addition, we note that

$$\langle\tilde{\epsilon}\epsilon_m\rangle=0\ , \tag{50b}$$

and that

$$\langle\tilde{\epsilon}(Q)\epsilon(-Q')\rangle=\delta_{\vec{Q}\,\vec{Q}'}k_BTV^{-1}\chi_0(Q)\ . \tag{50c}$$

The exact form of the function $\chi_0(Q)$ is not of interest.

B. The quasielastic scattering matrix

The Mueller matrix describing quasielastic scattering in the disordered phase can be obtained by appropriate modifications of the results given in Sec. II B for the case of an ordered polycrystalline specimen. The necessary changes in (16)—(18) are (a) the replacing of ϵ_m^2 and $\tilde{\epsilon}^2$ by their thermodynamic averages, as given in (50), and (b) the calculation of the prefactor $\tilde{g}^2$ for the disordered phase. This prefactor can, as before, be obtained by comparison with the Debye-Scherrer expression (20), where it is now understood that $\bar{N}$, is the number of diffracting planes scattering the incident beam into the angle between 2θ and $2(\theta+d\theta)$ is given by

$$\bar{N}=[V/(2\pi)^3]4\pi Q^2 dQ \ ; \tag{51a}$$

ρ, the density of unit cells, is simply $\rho=1/V$; i.e., we regard the entire specimen as a single unit cell; $|F|^2$ in (20) is replaced by its thermodynamic average $\langle |F^2| \rangle$. Using Bragg's law, $Q=4\pi s/\lambda$, (51a) becomes

$$\bar{N}=16\pi V s^2 c/\lambda^3) d(2\theta) \ . \tag{51b}$$

Instead of (22), we have

$$V^2\langle \tilde{\epsilon}^2 \rangle=(n^2\lambda^2/\pi)(e^2/mc^2)^2\langle |F| \rangle^2 \ . \tag{52}$$

Using $dl=r\,d\phi$, we obtain, from (20), (51b), and (52),

$$dP/d(2\theta)d\phi=r\Phi_1$$
$$=I_1(\pi^2V^2/2n^4\lambda^4)\langle \tilde{\epsilon}^2 \rangle(1+c_2^2) \ . \tag{53}$$

Comparing (53) and (19) (with $\tilde{g}$ now replaced by $\tilde{g}_d$ for the disordered phase) we obtain

$$\tilde{g}_d^2=\pi^2V^2/rn^4\lambda^4 \ . \tag{54}$$

Equations (17b) (with ϵ_m^2, $\tilde{\epsilon}^2$ replaced by their thermodynamic averages), (18) (with $\tilde{g}$ replaced by $\tilde{g}_d$), and (54) are the central results for scattering in the disordered phase.

A particularly interesting quantity to evaluate in the isotropic phase is the *difference* between the amount of light scattered by left- and right-circularly polarized incident radiation. This quantity has been measured by Meiboom and Sammon[2(b)] in amorphous BPIII, where the strongly selective nature of the scattering is the most prominent feature. The simplest possible explanation of this behavior would be to ascribe it to enhanced scattering, which is expected in the isotropic phase as the clearing point is approached from above. This would, of course, imply that BPIII is *not* a distinct thermodynamic phase, but rather a subregion of the isotropic one.

We thus wish to calculate

$$d\psi/d(2\theta)d\phi=r[(\Phi_1-\Phi_4)-(\Phi_1+\Phi_4)]$$
$$=\frac{1}{8}\frac{\pi^2V^2}{n^4\lambda^4}2|\tilde{\mu}_{14}|I_0 \ ,$$
$$=\frac{\pi^2}{2n^4\lambda^4}s(s^2+1)$$
$$\times[\langle \epsilon_2^2 \rangle-\langle \epsilon_{-2}^2 \rangle]I_0 \ , \tag{55}$$

where I_0 is the (equal) intensity of the incident circularly polarized beams, and $\tilde{\mu}_{14}$ is taken from (17b) with the changes previously noted. From (50a) we have

$$\langle \epsilon_{\pm 2}^2 \rangle=k_BTV^{-1}(a\mp 2dQ+c_1Q^2)^{-1} \ . \tag{56}$$

Using Bragg's law $Q=4\pi s/\lambda$ and the reduced variables[13(g),13(h)]

$$Q_C=d/c_1=4\pi/\lambda_C, \quad \tfrac{1}{4}t=(3\gamma/\beta^2)a \ ,$$
$$\tfrac{1}{4}\xi_R^2=(3\gamma/\beta^2)c_1 \ , \tag{57}$$
$$\eta=\lambda_c/\lambda, \quad \kappa=Q_C\xi_R \ ,$$

(56) becomes

$$\langle \epsilon_{\pm 2}^2 \rangle=k_BTV^{-1}(12\gamma/\beta^2)(t\mp 2\eta\kappa^2 s+\eta^2\kappa^2 s^2)^{-1} \ . \tag{56'}$$

Note that the reduced temperature

$$t=(T_{IC}-T_0)/(T_R-T_0)=\Delta T_{IC}/\Delta T_R \ ,$$

where T_{IC} and T_R are the isotropic-cholesteric and racemic-mixture transition temperatures, respectively, and T_0 is extrapolated from the disordered phase transition temperature for the racemic mixture.[13(h)] Substituting (56') into (55) and integrating over all scattering angles $0\le 2\theta\le\pi$, $0\le\phi\le 2\pi$ gives

$$\psi/I_0=(96\pi^3\eta\kappa^2\gamma k_BTV/n^4\lambda^4\beta^2)$$
$$\times\int_0^1 dv\frac{v(1+v)}{(t+\eta^2\kappa^2 v)^2-4\eta^2\kappa^4 v} \ , \tag{58}$$

with $v=s^2$. Carrying out the integration gives

$$\psi/I_0=(6\pi\gamma k_BTV/n^4\lambda_C^2\xi_R^2\beta^2)f(\eta,\tau=t/\kappa^2) \ , \tag{59}$$
$$f(\eta,\tau)=\eta+[(4-2\tau+\eta^2)/2\eta]\ln[(\tau+2\eta+\eta^2)(\tau-2\eta+\eta^2)/\tau^2]$$
$$+\{[\tau^2-\tau(8+\eta^2)+2(4+\eta^2)]/2\eta(\tau-1)^{1/2}\}\{\tan^{-1}[(\tau-2+\eta^2)/2(\tau-1)^{1/2}]$$
$$-\tan^{-1}[(\tau-2)/2(\tau-1)^{1/2}]\} \ .$$

A convenient way of eliminating the various parameters appearing in (59) is to relate ψ/I_0 to the magnitude of the step observed[2] in the transmitted light intensity in the cholesteric helicoidal phase at $\lambda=\lambda_C$. Considering only the dominant ϵ_2^2 contribution, we use (32b) with $\lambda=\lambda_C$ and $N=2$. For ϵ_2^2, we take the intensity immediately below the isotropic-cholesteric transition (i.e., we ignore the narrow temperature interval occupied by blue phases) and relate it to the latent heat (in energy/volume K) associated

with this transition by using the Landau-theory result[13(h)]

$$L=2T_{IC}\epsilon_2^2\frac{(\partial a/\partial T)_{T=T_{IC}}}{2+(1+\frac{1}{3}\kappa^2)^{1/2}} . \tag{60}$$

Since

$$\Delta T_{IC}/T_{IC}\ll 1$$

we have

$$(\partial a/\partial T)_{T=T_{IC}}\simeq a/\Delta T_{IC}=(\beta^2/12\gamma)t/\Delta T_{IC}$$
$$=(\beta^2/12\gamma)/\Delta T_R , \tag{61}$$

and, from (32b), we obtain

$$\Delta\Phi_T(\lambda=\lambda_C)_1/I_1$$
$$=\frac{3\pi^2[2+(1+\frac{1}{3}\kappa^2)^{1/2}]\gamma VL\Delta T_R}{n^4\lambda_C T_{IC}\beta^2} . \tag{62}$$

Setting $T=T_{IC}$ in (59), we finally have

$$R\equiv\frac{\psi/I_0}{\Delta\Phi_T(\lambda_C)_1/I_1}$$
$$=\frac{2(k_BT_{IC})(T_{IC}/\Delta T_R)}{\pi[2+(1+\frac{1}{3}\kappa^2)^{1/2}]L\lambda_C\xi_R^2}$$
$$\times f(\eta=\lambda_c/\lambda;\tau=t_{IC}/\kappa^2) , \tag{63}$$

with[13(h)]

$$t_{IC}=\tfrac{1}{2}[1+\kappa^2+(1+\tfrac{1}{3}\kappa^2)^{3/2}] , \tag{64}$$

for $\kappa\lesssim 3$, which is the region of interest.

A numerical estimate of R can be obtained as follows. We consider isotropic phase scattering in CN at a wavelength (in the material) of $\lambda=\lambda_c=230$ nm. A reasonable value for the racemic mixture correlation length ξ_R is 15 nm, which gives

$$\kappa=Q_c\xi_R=4\pi\xi_R/\lambda_c=0.82 .$$

Theoretical phase diagrams[13(h)] indicate that blue phases are observed for $\kappa\gtrsim 0.7$, so this is a reasonable value. For the other quantities appearing in (63) we take experimental values, $T_{IC}=365$ K, $\Delta T_R=0.5$ K, and $L=1$ J/cm^3−K. Substituting into (63), we obtain

$$R=5.2\times 10^{-3} ,$$

i.e., a $\frac{1}{2}\%$ effect. Since the experimentally observed[2(b)] BPIII selective scattering is 1–2 orders of magnitude greater than this, it is clear that it *cannot be ascribed to Ornstein-Zernike–type fluctuations in the isotropic phase as the clearing point is approached* and that alternate possibilities must therefore be explored.

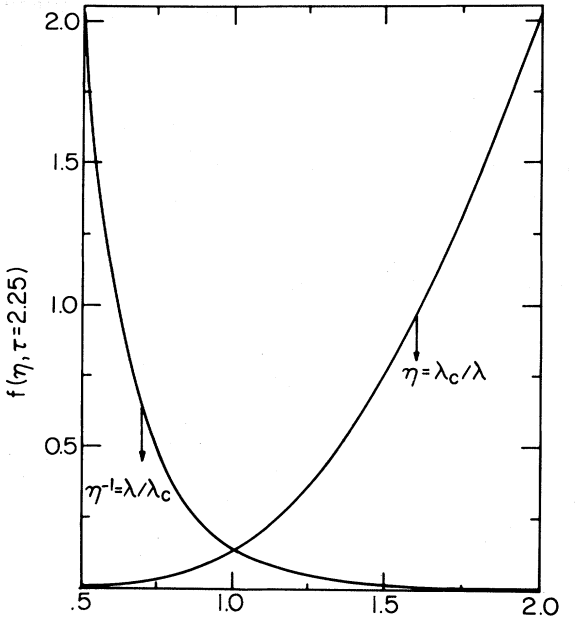

FIG. 3. Wavelength dependence of the difference in scattering intensity between right- and left-handed circularly polarized light, for quasielastic scattering in the isotropic phase just above the clearing point.

Finally, in Fig. 3, we illustrate the wavelength (λ) dependence of ψ/I_0, again taking $\kappa=0.82$. Clearly, the quasielastic scattering in the isotropic phase immediately above the clearing point increases as λ/λ_C decreases below unity. However, experimental results[2(b)] for BPIII show a stronger temperature dependence than that in Fig. 3, again indicating that the anomalous scattering observed in this phase cannot be ascribed to simple fluctuations in the disordered phase. We shall return to this point in the final section.

IV. DISCUSSION

In this paper we have presented a detailed description of elastic light scattering in cholesteric liquid-crystal systems. Our analysis was carried out within the framework of the Landau theory of phase transitions in cholesterics, which had been given elsewhere.[13(h)] Stressed particularly was the importance of analyzing the polarization characteristics of scattered light in cholesteric systems for arbitrarily polarized incident radiation, and how such measurements are related to the structural properties of cholesteric blue phases.

Our analysis utilized the Mueller matrix formalism, in which the scattering properties of the medi-

um are described by a 4×4 matrix which relates the 1×4 Stokes vectors of the scattered and incident beams. For the ordered blue phases, we first considered the case of scattering by a polycrystalline specimen (Debye-Scherrer—type configuration) in the Born approximation. The calculated Mueller matrix was compared with the experimental results of Flack *et al.*[3(d)] The agreement was quite good, particularly when the effect of optical activity was taken into account. Considering only the contribution of the dominant Fourier component of the order parameter to the theoretical Mueller matrix, the calculated results were within a few percent of the experimental intensity ratios. This, of course, indicates that higher-order contributions, which are important for understanding the detailed structure of the blue phase, may be difficult to detect with high accuracy in this particular configuration. For this reason, we also presented an analysis of scattering by a single-crystal specimen and showed that in this case the effect of higher-order terms is significantly greater. However, in practice elastic scattering measurements on single crystals present difficulties, due to extinctions and similar effects and considerable care must be taken.

We also compare (see Fig. 2) our theoretical results with the transmission versus wavelength measurements of Meiboom and Sammon[2(b)] on BPI. By fitting the first three Bragg magnitudes to the experimental data, we showed that the theoretical expression describes the measured intensity satisfactorily over the entire wavelength region studied.

In Sec. III, we studied quasielastic scattering in the isotropic phase, considering only quadratic (harmonic) fluctuations of the order parameter. Once again the Mueller matrix approached was used so as to obtain results for arbitrary polarization of the incident radiation. One of our objectives was to determine whether the strong anomalous scattering associated with BPIII [Ref. 2(b)] could be attributed to harmonic fluctuations of the order parameter in the vicinity of the clearing point. We find that this is probably not so since the observed BPIII scattering is 1—2 orders of magnitude *greater* than the theoretical estimate. In addition, the observed temperature dependence is much stronger than that calculated in the harmonic approximation. We therefore conclude that it is necessary to consider in greater detail two alternative explanations. (1) BPIII may in fact be a distinct thermodynamic phase which, however, is not characterized by periodic orientational order (i.e., it has the characteristics of a "glassy" state). One possibility for such a phase, the condensation of a collection of disordered, randomly oriented rodlike entities, has been previously suggested elsewhere.[13(g)] (2) Alternately, the harmonic approximation employed in Sec. III might be inadequate near the clearing point. In principle, there exist low-lying *localized* excitations in the disordered phase[13(g)] and these could result in enhanced light scattering having the characteristics observed in BPIII. In the latter case, BPIII would, of course, not be a distinct thermodynamic phase.

One possible way of distinguishing between these two possibilities is by inelastic-light-scattering studies. Utilizing such techniques, one can measure the lifetime of the light scatterers in BPIII. By comparing the results obtained with those of similar measurements on BPI and BPII it should be possible to determine whether the BPIII phase scatterers have a static or dynamic character. The former would indicate that BPIII is indeed a glassylike state while the latter would tend to confirm that localized excitations are responsible for the observed anomalous behavior.

Finally, we mention one additional experimental possibility for studying blue phases with long-range order. By using a coherent light source and holographic techniques one can, in principle, measure the relative *phases* as well as the amplitudes of the Bragg peaks. As we have noted, these phases are directly related to possible structure assignments and thus such measurements could provide a unique means of determining the structures of cholesteric blue phases.

ACKNOWLEDGMENT

We are grateful to many colleagues, including, particularly, S. Alexander, D. Mukamel, and M. Kugler, for useful discussions and comments. We also thank P. P. Crooker, P. H. Keyes, Z. Luz, M. Marcus, S. Meiboom, and H. Stegemeyer for keeping us apprised of their experimental results prior to publication and for helpful clarifications. This work was supported in part by a grant from the U. S.-Israel Binational Science Foundation (BSF), Jerusalem, Israel.

---

[1]For a review and references to earlier work, see H. Stegemeyer and K. Bergmann, in *Liquid Crystals of One- and Two-Dimensional Order,* edited by W. Helfrich and G. Heppke (Springer, Berlin, 1980), p. 161.

[2](a) S. Meiboom and M. Sammon, Phys. Rev. Lett. 44, 882 (1980); (b) Phys. Rev. A 24, 468 (1981).

[3](a) D. L. Johnson, J. H. Flack, and P. P. Crooker, Phys. Rev. Lett. 45, 641 (1980); (b) J. H. Flack and P. P.

Crooker, Phys. Lett. 82A, 247 (1981); (c) Mol. Cryst. Liq. Cryst. 69, 281 (1981); (d) J. H. Flack, P. P. Crooker, and R. C. Svoboda, Phys. Rev. A 26, 723 (1982).

[4]E. T. Samulski and Z. Luz, J. Chem. Phys. 73, 142 (1980).

[5](a) P. H. Keyes, A. J. Nicastro, and E. M. McKinnon, Mol. Cryst. Liq. Cryst. 67, 59 (1981); (b) A. J. Nicastro and P. H. Keyes, Phys. Rev. A 27, 431 (1983).

[6]D. Armitage and R. J. Cox, Mol. Cryst. Liq. Cryst. Lett. 64, 41 (1980).

[7](a) M. Marcus, J. Phys. (Paris) 42, 61 (1981); (b) Phys. Rev. A 25, 2272 (1982); (c) 25, 2276 (1982); (d) M. Marcus and J. W. Goodby, Mol. Cryst. Liq. Cryst. Lett. 72, 297 (1982); (e) M. Marcus, *ibid.* 82, 33 (1982); (f) 82, 167 (1982).

[8]T. K. Brog and P. J. Collings, Mol. Cryst. Liq. Cryst. 60, 65 (1980).

[9]P. L. Finn and P. J. Cladis, Mol. Cryst. Liq. Cryst. Lett. 72, 107 (1981); Mol. Cryst. Liq. Cryst. 84, 159 (1982).

[10]J. Her, B. B. Rao, and J. T. Ho, Phys. Rev. A 24, 3272 (1981); J. Her and J. T. Ho, in *Liquid Crystals and Ordered Fluids,* edited by A. C. Griffin and J. F. Johnson (Plenum, New York, 1982), Vol. 4.

[11](a) H. Onusseit and H. Stegemeyer, Z. Naturforsch. 36a, 1083 (1981); (b) Chem. Phys. Lett. 89, 95 (1982); (c) H. Stegemeyer and P. Pollmann, Mol. Cryst. Lett. 82, 123 (1982).

[12]M. S. Beevers, D. A. Elliott, and G. Williams, Mol. Cryst. Liq. Cryst. 80, 135 (1982).

[13]R. M. Hornreich and S. Shtrikman, (a) Bull. Israel Phys. Soc. 25, 46 (1979); (b) J. Phys. (Paris) 41, 335 (1980); 42, 367(E) (1981); (c) in *Liquid Crystals of One- and Two-Dimensional Order,* Ref. 1, p. 185; (d) Phys. Lett. 82A, 345 (1981); (e) Phys. Rev. A 24, 635 (1981); (f) Phys. Lett. 84A, 20 (1981); (g) R. M. Hornreich, M. Kugler, and S. Shtrikman, Phys. Rev. Lett. 48, 1404 (1982); (h) H. Grebel, R. M. Hornreich, and S. Shtrikman, Phys. Rev. A (in press).

[14]S. Alexander, in *Symmetries and Broken Symmetries in Condensed Matter Physics,* edited by N. Boccara (IDSET, Paris, 1981), p. 141.

[15]W. Kuczynski, K. Bergmann, and H. Stegemeyer, Mol. Cryst. Liq. Cryst. 56, 283 (1980); H. Stegemeyer, Phys. Lett. 79A, 425 (1980).

[16]H. Schröder, in *Liquid Crystals of One- and Two-Dimensional Order,* Ref. 1, p. 196.

[17](a) H. Kleinert, Phys. Lett. 81A, 141 (1981); (b) H. Kleinert and K. Maki, Fortschr. Phys. 29, 219 (1981).

[18]S. Meiboom, J. P. Sethna, P. W. Anderson, and W. F. Brinkman, Phys. Rev. Lett. 46, 1216 (1981); S. Meiboom, M. Sammon, and W. F. Brinkman, Phys. Rev. A 27, 438 (1983); M. Sammon, Mol. Cryst. Liq. Cryst. (in press).

[19]D. Bensimon, E. Domany, and S. Shtrikman, Phys. Rev. A (in press).

[20]Introductions to the Mueller matrix can be found in H. C. van de Hulst, *Light Scattering by Small Particles* (Wiley, New York, 1957); A. Gerrard and J. M. Burch, *Introduction to Matrix Methods in Optics* (Wiley, New York, 1975); W. A. Shurcliff, *Polarized Light* (Harvard University Press, Cambridge, Mass., 1962). For an application of this approach, see R. C. Thompson, J. R. Bottiger, and E. S. Fry, Appl. Opt. 19, 1323 (1980).

[21]L. D. Landau and E. M. Lifshitz, *Statistical Physics,* 3rd ed. (Pergamon, Oxford, 1980), Chap. 14.

[22]Certain relationships exist between the 16 elements of the Mueller matrix (in general, inequalities). See E. S. Fry and G. W. Kattawar, Appl. Opt. 20, 2811 (1981); 21, 18 (1982).

[23]R. Pepinsky and V. Vand, in *Handbook of Physics,* edited by E. U. Condon and H. Odishaw (McGraw-Hill, New York, 1958), pp. 8—15.

[24]P. G. de Gennes, Mol. Cryst. Liq. Cryst. 12, 193 (1971).

[25]S. A. Brazovskii and S. G. Dmitriev, Zh. Eksp. Teor. Fiz. 69, 979 (1975). [Sov. Phys. JETP 42, 497 (1976)]; S. A. Brazovskii and V. M. Filev, *ibid.* 75, 1140 (1978) [*ibid.* 48, 573 (1978)].